AD NUMBER

AD482931

LIMITATION CHANGES

TO:

Approved for public release; distribution is unlimited.

FROM:

**Distribution authorized to U.S. Gov't. agencies and their contractors;
Administrative/Operational Use; 28 OCT 1965.
Other requests shall be referred to Defense Advanced Research Projects Agency, 675 North Randolph Street, Arlington, VA 22203-2114.**

AUTHORITY

SAMSO ltr, 28 Feb 1972

RN-28, October 1965

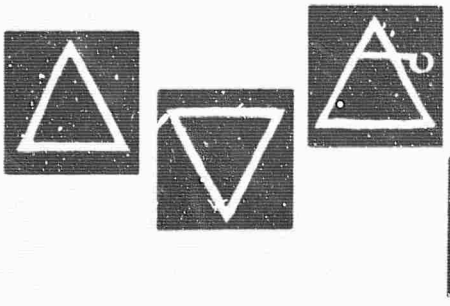

ELECTRO-OPTICAL SYSTEMS, INC.
RESEARCH NOTES

A FINITE DIFFERENCE METHOD FOR SOLVING THE LAMINAR BOUNDARY LAYER EQUATIONS NEAR A WAKE NECK

Eric Baum

Handed down from the Middle Ages, these mystic symbols were representative of the four elements in nature: ◬ air, ▽ water, ▽ earth, and △ fire. Modern science has since identified these four elements with the four states in which matter appears in the universe: gas, liquid, solid, and plasma. Understanding the properties of matter in these four forms is the basis of modern and future technology.

EOS Research Note No. 28, October 1965

A FINITE DIFFERENCE METHOD FOR SOLVING THE LAMINAR BOUNDARY LAYER EQUATIONS NEAR A WAKE NECK

Eric Baum

EOS

ELECTRO-OPTICAL SYSTEMS, INC. Pasadena, California

A Subsidiary of Xerox Corporation

ABSTRACT

A laminar wake model is studied which assumes that the boundary layer equations are valid in a shear layer on the axis of symmetry, and that the local pressure is determined by a displacement interaction with the inviscid outer flow. The finite difference method used places no restrictions on the shape of the velocity profile. The qualitative features of the solution are the same as those found by previous investigators using integral methods, in that an otherwise arbitrary initial condition (the local free stream Mach number) is determined by the fact that only a particular value results in a physically meaningful solution. Two methods of finding the particular solution are investigated.

This research is a part of PROJECT DEFENDER, sponsored by the Advanced Research Projects Agency, Department of Defense, under ARPA Order No. 254-62, monitored by Air Force Ballistic Systems Division under Contract AF04(694)-570.

TABLE OF CONTENTS

ILLUSTRATIONS

ACKNOWLEDGMENT

The author wishes to express his appreciation to M.R. Denison for his encouragement and for many useful discussions during the c se of this work.

A Finite Difference Method for Solving the Laminar Boundary Layer Equations Near a Wake Neck

INTRODUCTION

The qualitative features of the base flow region of supersonic blunt-based bodies, shown schematically in Fig. 1, have been recognized for many years. Much of the early work was aimed at determining the base pressure, and it was generally agreed, long before any quantitative theory was available, that an interaction between the shear layer and the outer inviscid flow was important in determining its value. The Crocco-Lees[1] mixing theory put this on a somewhat more quantitative basis. The model on which this theory is based assumes that the boundary layer equations are valid in the shear layer and that the local pressure is determined by a displacement interaction with the inviscid outer flow. The effects of the shear layer profiles are lumped into variables which must be determined independently, so that the theory is incomplete. However, the qualitative results show what behavior to expect from a more rigorous solution of the same model. They found that there were an infinite number of solutions to the equations, corresponding to all possible choices of the base pressure. However, the only one with physical meaning was the singular solution passing through a saddle-point type of singularity. The most familiar example of this type of behavior is in the calculation of flow through a one dimensional nozzle. In that case, the governing equation is

$$\frac{dM}{dx} = - \frac{1}{A} \frac{dA}{dx} \frac{M\left(1 + \frac{\gamma-1}{2} M^2\right)}{(1 - M^2)}$$

which can of course be integrated in closed form. However, if one chooses to consider $\frac{1}{A} \frac{dA}{dX}$ as a specified function of x, one can solve the first order differential equation for any initial value of M.

1. L. Crocco and L. Lees, "A Mixing Theory for the Interaction Between Dissipative Flows and Nearly Isentropic Streams," J. Aer. Sci. 19, 649-676 (1952).

If the required solution is to have $M < 1$ in the converging section and $M > 1$ in the diverging section, then M must pass through 1 and $\frac{dA}{dx}$ through zero during the course of the calculation. If the initial choice of M is too small, $\frac{dA}{dx}$ will pass through zero first, after which $\frac{dM}{dx}$ becomes negative and the flow is subsonic everywhere in the nozzle. If the initial choice is too large $M \to 1$ first and the calculation terminates at M = 1, a solution with no physical meaning. The only solution which becomes supersonic in the diverging section corresponds to $\frac{dA}{dx} \to 0$ and $M \to 1$ simultaneously.

This analogy is useful in obtaining an understanding of the nature of the wake critical point, but it should not be carried too far. For example, the pressure increases as the flow approaches the wake critical point, indicating that the acceleration of the low speed portion of the flow is produced by viscous forces, which are not present in the one dimensional nozzle model. Relating the wake critical point to an average Mach number of unity is therefore not justified.

Recently, Reeves and Lees[2] investigated this wake model in more detail, using a two moment integral method to determine profile shape and wake thickness. To insure the proper qualitative features, the Stewartson[3] family of solutions to the Falkner-Skan equation, $f'(\frac{\eta}{\eta_\delta},\beta)$, was used to describe the profile shape, $\frac{u}{u_\delta}(\frac{\eta}{\eta_\delta},\gamma)$ with η_δ and γ determined by the zero and first moments of the momentum equation. Since a stagnation point on the centerline occurs for only a single value of γ, the shape of the profile at the wake stagnation point is arbitrarily predetermined by the choice of the Stewartson family and only the wake thickness at this point is calculated.

---

2. B. L. Reeves and L. Lees, "Theory of the Laminar Near Wake of Blunt Bodies in Hypersonic Flow" presented at AIAA 2nd Aerospace Sciences Meeting, New York, January 1965, AIAA Paper No. 65-52.

3. K. Stewartson, "Further Solutions of the Falkner Skan Equation," Proc. Comb. Phil. Soc. 50, 454-465 (1954).

Webb, Golik, Vogenitz and Lees[4] investigated the model using the polynomial profiles

$$\frac{u}{u_\delta} = \frac{u_c}{u_\delta} + \left(1 - \frac{u_c}{u_\delta}\right) \left[3\left(\frac{\eta}{\eta_\delta}\right)^2 - 2\left(\frac{\eta}{\eta_\delta}\right)^3\right]$$

and

$$\frac{u}{u_\delta} = \frac{u_c}{u_\delta} + \left(1 - \frac{u_c}{u_\delta}\right) \left[2\left(\frac{\eta}{\eta_\delta}\right)^2 - \left(\frac{\eta}{\eta_\delta}\right)^4\right]$$

in which a two moment method was used to find $\frac{u_c}{u_\delta}$ and η_δ. He e, again the profile shape at the wake stagnation point is predetermined by the choice of profile families. They then went one step further and used the Stewartson family $f'(\frac{\eta}{\eta_\delta}, \beta)$ to describe profile shape, using the following substitutions:

$$f' \rightarrow (u-u_c)/(u_\delta - u_c)$$

$$\frac{\eta}{\eta_\delta} \rightarrow \frac{\eta}{\eta_\delta}$$

$$\beta \rightarrow \gamma$$

where $\frac{u_c}{u_\delta}$ is now no longer related to γ. The third parameter was found using an additional moment of the momentum equation.

The biggest drawback of the integral methods is that in order to get accurate results, the family of profiles chosen mus be capable of a reasonably good representation of the actual profiles over the entire range of calculation. Since the actual profiles are not generally known in advance, this requires the exercise of a considerable degree of judgment and intuition on the part of the investigator. In this particular problem, there is the additional obstacle of a gap between the body boundary layer and the neighborhood of the rear stagnation point, in which the boundary layer equations alone are clearly inadequate in describing the flow between the centerline and the outer inviscid flow.

4. W.H. Webb, R.J. Golik, F.W. Vogenitz and Lester Lees, "A Multimoment Integral Theory of the Laminar Supersonic Near Wake," Proc., 1965 Heat Transfer and Fluid Mechanics Institute, p. 168, Stanford U. Press, Stanford, Calif., 1965.

Since a different method of calculation is required in this region, it is not likely that the profiles approaching the rear stagnation point will fit smoothly into a prechosen family, and it is not possible to base an integral method calculation on an arbitrary initial profile.

This paper describes a finite difference method for solving the boundary layer equations with the local pressure determined by a displacement interaction with the outside inviscid flow. There are no constraints on profile shape, and the calculation begins with an arbitrary profile at the wake stagnation point and proceeds downstream. The solutions are found to fall into two families, depending on whether the initial local inviscid Mach number is smaller or larger than the value corresponding to a singular solution. If the Mach number is smaller than this eigenvalue, the wake centerline velocity increases for only a short distance downstream, then decreases again until another stagnation point is reached, the flow past this point being in the direction of the body. If the initial local inviscid Mach number is larger than the eigenvalue, the shear layer thickness decreases at an accelerating rate, until the inviscid flow intersects the axis as the shear layer disappears. Both of these types of behavior are valid solutions to the equations, but only the singular solution has the appropriate downstream behavior, that is, the wake velocity approaches the local freestream value.

EQUATIONS

The coordinate system as shown in Fig. 1 employs distances measured along the centerline and normal to it. The origin is at the base flow rear stagnation point. The calculations will be limited here to two dimensional, adiabatic, ideal gas, flow. The continuity and momentum equations

$$\frac{\partial \rho u}{\partial x} + \frac{\partial \rho v}{\partial y} = 0 \qquad (1)$$

$$\rho u \frac{\partial u}{\partial x} + \rho v \frac{\partial u}{\partial y} = \frac{\partial}{\partial y} \mu \frac{\partial u}{\partial y} - \frac{dP}{dx} \qquad (2)$$

can be transformed into the form

$$u^* \frac{\partial u^*}{\partial S^*} + v^* \frac{\partial u^*}{\partial Y^*} - \frac{\partial^2 u^*}{\partial Y^{*2}} = - \frac{dP}{dS^*} \cdot \frac{1}{\rho_e u_e^2} \left[\frac{\rho_e}{\rho} - u^{*2} \right] \qquad (3)$$

where $u^* = u/u_e$, e denoting conditions at shear layer edge.

$$v^* = - \left(\frac{\partial \psi^*}{\partial S^*} \right)_Y$$

$$\psi^* = \frac{1}{\sqrt{S_b}} \int_o \rho u dy$$

$$Y^* = \frac{1}{\sqrt{S_b}} \int_o^y \rho u_e dy$$

$$S^* = \frac{1}{S_b} \int_o^x C \rho_e u_e \mu_e dx \quad \text{where } C = \frac{\rho \mu}{\rho_e \mu_e}$$ (Chapman-Rubesin parameter, assumed to be a function of x only)

S_b = scale factor making equation dimensionless

For ideal gas conditions, the right side of Eq. (3) can be written

$$- \frac{dP}{dS^*} \frac{1}{\rho_e u_e^2} \left[\frac{\rho_e}{\rho} - u_*^2 \right] = \frac{1}{M_e} \frac{dM_e}{dS^*} (1 - u_*^2) \tag{4}$$

It is convenient, now, to further transform Eq. (3) into a less familiar form, with dependent variable

$$G = \left(\frac{\partial u^*}{\partial Y^*} \right)^2 \tag{5}$$

and independent variables S^* and $\bar{u}$, where

$$\bar{u} = \frac{u^* - u_c^*}{1 - u_c^*}, \text{ c denoting conditions at the centerline} \tag{6}$$

$$\left[u^* \right] \frac{\partial G}{\partial S^*} = \left\{ \frac{G}{(1 - u_c^*)^2} \right\} \frac{\partial^2 G}{\partial \bar{u}^2} + \left\{ \left[\frac{u^*(1 - u^*)}{(1 - u_c^*)} \frac{du_c^*}{dS^*} - \frac{1}{2(1-u_c^*)} \frac{\partial G}{\partial \bar{u}} - \frac{1}{M_e} \frac{dM_e}{dS^*} (1-u^{*2}) \right] \cdot \frac{1}{(1 - u_c^*)} \right\} \frac{\partial G}{\partial \bar{u}} - \left[\frac{4}{M_e} \frac{dM_e}{dS^*} u^* \right] G \tag{7}$$

The boundary conditions appropriate to a wake are $G(o) = G(1) = 0$.

The fixed location of the boundaries in the $\bar{u}$ coordinate greatly simplify the application of the finite difference method, and the use of G instead of $\frac{\partial u^*}{\partial Y^*}$ as dependent variable makes it more convenient to satisfy the differential equation at the centerline, where Eq. (7) reduces to

$$u_c^* \frac{du_c^*}{dS^*} = \frac{1}{2(1 - u_c^*)} \left(\frac{\partial G}{\partial \bar{u}} \right)_c + \frac{1}{M_e} \frac{dM_e}{dS^*} (1 - u_c^{*2})$$

Here since $\frac{1}{2}\left(\frac{\partial G}{\partial \bar{u}}\right)_c = \left(\frac{\partial u^*}{\partial Y}\right)_c \left(\frac{\partial}{\partial \bar{u}} \frac{\partial u^*}{\partial Y}\right)_c$, the advantage in using G as the dependent variable becomes clear when it is realized that, while $\left(\frac{\partial u^*}{\partial Y}\right)_c$ is zero, $\left(\frac{\partial}{\partial \bar{u}} \frac{\partial u^*}{\partial Y}\right)_c$ is infinite so that $\left(\frac{\partial G}{\partial \bar{u}}\right)_c$ generally has a finite value.

Equation (7) is in a modified form of the Crocco coordinate system and, as is well known, solutions to the boundary layer equations in these coordinates are not unique, in that a single solution in the Crocco coordinates contains an infinite number of distinct solutions in the physical coordinates. This occurs because the usual third boundary condition (the location of a reference streamline) of the momentum equation in physical coordinates cannot be imposed in the Crocco coordinates, and the solutions corresponding to all possible values of this boundary condition map into a single Crocco solution. We wish, here, to remove the ambiguity of the solution of Eq. 7 by imposing the condition that the centerline ($\bar{u} = 0$) is a streamline. Of the many possible ways of accomplishing this, we choose to use an integral of the momentum equation, with $\left(\frac{\partial \psi}{\partial S}\right)_Y$ set equal to zero at Y = 0:

$$\frac{d}{dS^*}\left[(1 - u_o^*)\int_o^1 u^* (1 - u^*) \frac{d\bar{u}}{\sqrt{G}}\right] = -\frac{1}{M_e}\frac{dM_e}{dS^*}(1 - u_c^*)\int_o^1 (1 - u^{*2}) \frac{d\bar{u}}{\sqrt{G}} \tag{8}$$

An additional relation between $\frac{du_c^*}{dS^*}$ and $\frac{1}{M_e}\frac{dM_e}{ds}$ is required in order to complete the specification of the problem. This is obtained from an integrated form of the continuity equation:

$$\frac{v_e}{u_e} = \frac{d\delta^*}{dx} - \frac{d\ \ell n\ \rho_\delta u_\delta}{dx}\int_o^\delta \frac{\rho u}{\rho_\delta u_\delta} dy = \tan\theta \tag{9}$$

where

$$\delta^* = \int_o^\delta \left(1 - \frac{\rho u}{\rho_\delta u_\delta}\right) dy \tag{10}$$

The logarithmic term in Eq. (9) is not bounded with increasing δ, and since δ is arbitrary, the inclusion of this term is difficult to justify within the framework of the boundary layer theory, and it will be neglected in these calculations.

Equation (9), when transformed into the coordinate system of Eq. (3), becomes

$$\frac{d}{dS^*}\left(\frac{\rho_\infty u_\infty \delta^*}{\sqrt{S_b}}\right) = \frac{\sqrt{S_b}}{\mu_\infty} \cdot \frac{M_\infty}{M_e}\left(\frac{1+\frac{\gamma-1}{2}M_e^2}{1+\frac{\gamma-1}{2}M_\infty^2}\right)^{\frac{\gamma}{\gamma-1}} \tan\theta \qquad (11)$$

where it has been assumed for simplicity that $\mu \sim T^{1/2}$. Subscript ∞ refers to a reference point in the flow, taken here to be at $\theta = 0$. The term $\frac{\sqrt{S_b}}{\mu_\infty}$ is like $\sqrt{Re}$. If the calculation were linked to a given body, it would be convenient to divide this into a conventional Reynolds number and a factor dependent primarily on body shape, but for the present we will define

$$Re = \frac{S_b}{\mu_\infty^2} \qquad (12)$$

A transformation of the displacement thickness definition, Eq. (10) into the coordinate system of Eq. (3) gives:

$$\frac{\rho_\infty u_\infty \delta^*}{\sqrt{S_b}} = (1-u_c^*)\frac{M_\infty}{Me}\left\{\left[\frac{1+\frac{\gamma-1}{2}M_e^2}{1+\frac{\gamma-1}{2}M_\infty^2}\right]^{\frac{\gamma+1}{2(\gamma-1)}}\int_0^1 (1-u^*)\frac{d\bar{u}}{\sqrt{G}} + \frac{\gamma-1}{2}M_e^2\int_0^1 (1-u^{*2})\frac{d\bar{u}}{\sqrt{G}}\right\} \qquad (13)$$

where, it should be noted, both of the shear layer integral functions are bounded.

A final relation is required between the local flow angle θ and local inviscid Mach number M_e. This could be obtained by means of a detailed calculation of the inviscid flow field, but for the purposes of these calculations, we will assume that this relation is given by the Prandtl-Meyer function:

$$\theta = \nu_\infty - \nu \tag{14}$$

The equations presented in this section, along with the appropriate initial conditions, completely specify the problem.

The momentum boundary layer equation (7) requires an initial G vs $\bar{u}$ profile, and auxilliary equations to evaluate u_c, $\frac{1}{M_e}\frac{dM_e}{dS^*}$ and $\frac{du_o}{dS^*}$. Equations (8), (11), (13) and (14) relate

$$\frac{du_c^*}{dS^*},\ \frac{1}{M_e}\frac{dM_e}{dS^*},\ \frac{d\left(\frac{\rho_\infty u_\infty \delta^*}{\sqrt{S_b}}\right)}{dS^*},\ u_c^*,\ M_e,\ \frac{\rho_\infty u_\infty \delta^*}{\sqrt{S_b}},\ \text{and } \theta$$

If θ is eliminated between Eqs. (14) and (11) and equation (13) is differentiated the three remaining equations could be thought of as simultaneous ordinary differential equations for u_c^*, M_e and $\frac{\rho_\infty u_\infty \delta^*}{\sqrt{S_b}}$, where only two initial conditions are arbitrary because Eq. (13) provides a relation between these and the third. Since one would normally know u_c^* if he knows the initial G vs. $\bar{u}$ profile, we will consider $(u_c^*)_{\text{initial}}$ to be fixed, and then arbitrarily let $\left(\frac{\rho_\infty u_\infty \delta^*}{\sqrt{S_b}}\right)_{\text{initial}}$ be specified by Eq. (13), leaving $(M_e)_{\text{initial}}$ as yet undetermined. M_{eo} will then be the eigenvalue and will be chosen so that the solution far downstream has the appropriate behavior.

METHOD OF SOLUTION

The momentum equation (7) can be solved readily by the use of an implicit finite difference method, with the accuracy limited only by the available computing time and computer memory size. Initial conditions are unrestricted except for the requirement that they satisfy the boundary conditions and not contain discontinuities. Exceptions to these requirements can be successfully treated by using local analytical solutions, but we do not expect any such cases to arise in the current problem. The method uses the following finite difference approximations for the linear (not bracketed) terms in Eq. (7):

$$\frac{\partial G}{\partial S} = (G_{i,\,j+1} - G_{i,j}) \,/\, \Delta S \tag{15}$$

$$\frac{\partial^2 G}{\partial \bar{u}^2} = (G_{i+1,j+1} + G_{i+1,j} - 2\,(G_{i,j+1} + G_{i,j}) + G_{i-i,j+1} + G_{i-i,j})/2\Delta \bar{u}^2$$

$$\frac{\partial G}{\partial \bar{u}} = (G_{i+1,j+1} + G_{i+1,j} - G_{i-1,j+1} - G_{i-1,j}) \,/\, 4\Delta \bar{u} \tag{17}$$

$$G = (G_{i,j+1} + G_{i,j})/2 \tag{18}$$

where i refers to the $\bar{u}$ coordinate
j refers to the S coordinate

The bracketed terms are evaluated at i,j for an initial iteration, then averaged between i,j and i,j+1 for succeeding iterations until they converge to a limiting value. If N interior meshpoints in $\bar{u}$ are used, the

finite difference approximation to Equation (7) results in N simultaneous linear algebraic equations for the unknown $G_{i,j+1}$. The equation at each point refers to $G_{i+1,j+1}$ and $G_{i-1,j+1}$ and therefore the equations are coupled in such a way that the matrix of coefficients contains 3 bands consisting of the diagonal, and the bands immediately above and below the diagonal. Such a set of equations is very quickly and easily solved by Gaussian elimination.

The auxiliary equations are solved simultaneously with the momentum equation in the following sequence.

1. Guess $\left(\frac{du^*_c}{dS^*}\right)_{j+\frac{1}{2}}$
2. Calculate $u^*_{c_{j+1}}$
3. Solve the momentum equation, evaluating bracketed terms at j and using the previous $\frac{1}{M_e}\frac{dM_e}{dS^*}$ for the first iteration.
4. Calculate $\left(\frac{1}{M_e}\frac{dM_e}{dS^*}\right)_{j+1/2}$ from Eq. (8).
5. Repeat three and four using averaged values until converged.
6. Calculate Me_{j+1} by finite difference integration of $\frac{1}{M_e}\frac{dM_e}{dS}$.
7. Calculate $\left(\frac{\rho_\infty u_\infty \delta^*}{\sqrt{S_b}}\right)_{j+1}$ from Eq. (13).
8. Evaluate $\frac{d}{dS^*}\left(\frac{\rho_\infty u_\infty \delta^*}{\sqrt{S_b}}\right)_{j+1/2}$ from Eq. (11)
9. Compare the finite difference derivative

$$\left[\left(\frac{\rho_\infty u_\infty \delta^*}{\sqrt{S_b}}\right)_{j+1} - \left(\frac{\rho_\infty u_\infty \delta^*}{\sqrt{S_b}}\right)_j\right]/\Delta S$$

with that evaluated in Step 8.

10. Use a systematic iteration procedure to guess a new $\left(\frac{du_c^*}{dS^*}\right)_{j+1/2}$ which will give better agreement than in step 9 and repeat from Step 1 to convergence.

The modified Newton's method used for iterating on $\left(\frac{du_c^*}{dS^*}\right)_{j+1/2}$ generally converges to 5 figures in about 4 iterations.

The principal drawback of the method is due to Step 9, where a finite difference derivative is required. In order for this difference to maintain significance, the profiles which determine δ^* must be considerably more accurate than one would normally require and the calculation therefore more time-consuming.

RESULTS

Typical results of this method of calculation are shown in Figs. (2) and (3). The initial profile used was, for convenience, one of the Stewartson family tabulated by Kennedy,[5] where $f''(f',\beta) \rightarrow \sqrt{G}\,(\bar{u},-.1988)$ with $R_2=10^6$ and $M_{e_\infty}=6$. Figure (2) shows the behavior of $\frac{du_c^*}{dS^*}$ corresponding to different assumed eigenvalues. When M_{eo} is too large, $\frac{du_c^*}{dS^*}$ begins to increase rapidly at some point in the calculation. This is accompanied by an increase in $\frac{1}{M_e}\frac{dM_e}{dS^*}$ toward infinity from its initially negative value, as shown in Fig. (3). The centerline velocity is therefore increasing rapidly at the same time that the inviscid flow just outside the shear layer is turning rapidly in toward the axis of symmetry. In the limit, the shear layer disappears entirely as the inviscid flow intersects the axis. This limit is reached at a finite distance downstream and constitutes a barrier past which the calculation cannot proceed. When the assumed eigenvalue M_{e_o} is too small, $\frac{du_c^*}{dS^*}$ becomes negative at some point in the calculation, after which the centerline velocity ratio decreases until a second stagnation point is reached, the flow on the centerline past this point having its origin downstream rather than upstream.

Only the eigen- solution belongs to neither of these two families of non-physical solutions. The source of this singular behavior can be more easily seen by differentiating equation (13), and combining with Eq. (11) to get an equation of the form:

$$a_1 \frac{dM_e}{dS^*} + a_2 \frac{du_c^*}{dS^*} = a_3 \qquad (19)$$

---

5. E.D. Kennedy, "Wake-Like Solutions to the Laminar Boundary Layer Equations," AIAA J. 2, 225-231 (1964).

where a_1, a_2 and a_3 contain no S* derivatives (the $\frac{\partial G}{\partial S^*}$ from the displacement thickness integrals can be eliminated by using the momentum equation). Equation (8) has the same form (again eliminating $\frac{\partial G}{\partial S^*}$ using the momentum equation):

$$b_1 \frac{dM_e}{dS^*} + b_2 \frac{du_c^*}{dS^*} = b_3 \tag{20}$$

and these two equations solved for $\frac{dM_e}{dS^*}$ and $\frac{du_c^*}{dS^*}$ give:

$$\frac{dM_e}{dS^*} = \frac{a_3 b_2 - a_2 b_3}{a_1 b_2 - a_2 b_1} = \frac{N_1}{D} \tag{21}$$

$$\frac{du_c^*}{dS^*} = \frac{a_1 b_3 - a_3 b_1}{a_1 b_2 - a_2 b_1} = \frac{N_2}{D} \tag{22}$$

Initially, N_2 and D have a like sign, N_1 the opposite sign. When M_{e_o} is too large, N_1 changes sign first, then D approaches zero so that $\frac{dM_e}{dS^*} \to \infty$, $\frac{du_c^*}{dS^*} \to \infty$. When M_{e_o} is too small, N_2 changes sign first and the centerline velocity decreases, then D approaches zero. The eigen solution has N_1 and D (and therefore N_2) changing sign simultaneously. It should be noted that if one of the equations (19) or (20) were to be eliminated by specifying either $\frac{dM_e}{dS^*}$ (S*) or $\frac{du_c^*}{dS^*}$ (S*), the singular behavior would no longer occur. This suggests an alternate method of solution of the equations which is described in Appendix I.

Of particular interest to those using the integral methods is the profile shape obtained by the finite difference method. A convenient way of presenting the shape is to plot G/G_{max} vs. $\bar{u}$, as in Fig. 4. The initial profile at the wake stagnation point ($u_c = 0$) and the calculated profile at $u_c = .3\ u_e$ are shown. The initial conditions coincide with one of the Stewartson family ($\beta = -.1988$). The shapes of other Stewartson profiles, also plotted in Fig. 4 ($\beta = -.40, -.50$) show clearly that this family very accurately represents the calculated non-similar pro-

files. However, it should be remembered that the use of a Stewartson profile shape at the wake stagnation point was arbitrary and there is some doubt that such a choice is realistic.

This study has shown that this particular viscous interaction problem can be solved in a straightforward manner using a finite difference method. A considerable effort has been made to extend the method of calculation to regions of reverse flow, without success. Several hybrid methods have been investigated, in which integrals of the conservation equations are used in the reverse flow region and finite differences are used elsewhere. All of these attempts failed because the profile shapes used for the integral method did not have the proper qualitative features. This sensitivity to the details of the profile shape in the reverse flow region was also pointed out by Webb, et al[4], who used a momentum integral method over the entire shear layer. The results of an integral method are in doubt whenever such sensitivity exists, so it appears that additional work is needed in the region between the body and the wake stagnation point before any quantitative results can be obtained from the interaction model.

APPENDIX I

INVERSE METHOD

Computing through a saddle point singularity is difficult even if the equations are simple in form since the eigenvalue can be found only to a limited number of significant figures. Assuming that one is then close enough to the critical point to make some kind of extrapolation valid, the calculation can be restarted on the other side and proceed from there without difficulty. However, when a partial differential equation is included in the set of equations, the computing time involved in this procedure can become excessive. A considerable saving in time would result from a method which did not require that such a large number of significant figures be carried.

The method which will be described here has this property, and consists essentially of guessing $\frac{du_c^*}{dS^*}(S^*)$ and solving the momentum equation, using Eq. (8) to give $\frac{1}{M_e}\frac{dM_e}{dS^*}$. The remaining auxiliary equations are not satisfied (that is $d(\frac{\rho_\infty u_\infty \delta^*}{\sqrt{S_b}})/dS^*$ from Eq. (11) does not agree with $\Delta(\frac{\rho_\infty u_\infty \delta^*}{\sqrt{S_b}})/\Delta S^*$ from Eq. (13), and a new guess of $\frac{du_c^*}{dS^*}(S^*)$ is made in such a way that agreement improves in succeeding iterations. There is no guarantee of convergence and the key to the method is, obviously, the type of iteration used.

For any given guess of $\frac{du_c^*}{dS^*}(S^*)$, the momentum equation and Eq. (8) can be solved for $G(\bar{u},S^*)$, $u_c^*(S^*)$ and $\frac{1}{M_e}\frac{dM_e}{dS^*}(S^*)$. The initial conditions required for this solution are $G(\bar{u},o)$ and $u_c^*(0)$. The values of $M_e(S^*)$ do not appear in these equations, so that $\frac{1}{M_e}\frac{dM_e}{dS^*}(S^*)$ is found without specifying M_e anywhere. The initial condition needed to integrate $\frac{1}{M_e}\frac{dM_e}{dS^*}(S^*)$ can therefore be applied at any value of S^*. The eigen-solution we are seeking has $M_e = M_{eo}$ at the origin and $M_e \to M_{e\infty}$ asymptotically far downstream. Since $M_{e\infty}$ is known, we will integrate $\frac{1}{M_e}\frac{dM_e}{dS^*}(S^*)$ in the upstream direction, assuming that the domain has been chosen large enough to make the asymptotic value of M_e reasonable at the downstream end. Since $M_e(\infty) \to M_{e\infty}$ only for the eigen-solution,

this means that if the procedure converges at all, it must converge to the desired solution.

The fact that the differential equation and $\frac{1}{M_e}\frac{dM_e}{dS^*}(S^*)$ are integrated in opposite directions introduces the major difficulty encountered in applying the method, since it makes it impractical to use a straightforward iteration scheme such as Newton's method. If they were integrated in the same direction, a local change in $\frac{du_c^*}{dS^*}$ would affect Eqs. 11 and 13 only downstream of the point, whereas, when they are integrated in opposite directions, the change is felt downstream due to the change in $\frac{du_c^*}{dS^*}$ and upstream due to the effect on all preceding values of M_e. The iteration method used was the simplest possible; a complete calculation was made using the current guess of $\frac{du_c^*}{dS^*}(S^*)$, and a second complete calculation was made using $1+\epsilon$ times the current guess (where $\epsilon \ll 1$). The results of these two calculations were used to make a point by point linear extrapolation to that value of $\frac{du_c^*}{dS^*}$ giving agreement between equations 11 and 13. All of the indicated changes in $\frac{du_c^*}{dS^*}$ were then reduced by a factor which decreased the largest fractional change to $\beta(\beta<1)$. There is no mathematical foundation for this iteration scheme, but a rigorous extrapolation is so much more difficult that it was decided to try this first. How well the method actually works is illustrated in Figure 5. The problem here is the same as the one used to demonstrate the direct method calculation, where the eigenvalue was found to be $M_{e_0} = 6.55$. The domain was taken to extend from $S^*=0$ to $S^*=1.5$ (at which point $M_e = M_{e_\infty} = 6.0$). The initial guess of $\frac{du_c^*}{dS^*}$ was taken to be 0.3 everywhere. Initially, values of $\beta = .2$, $\epsilon = .05$ were used. To speed convergence, β was changed to .05 after 8 iterations. About 15 iterations were required to find the eigen-value to the same number of significant figures as the direct method. The agreement after 20 iterations between $\frac{\rho_\infty u_\infty \delta^*}{\sqrt{s_5}}$ calculated from Eq. 11 with that calculated from Eq. 13 is shown in Fig. 6. This agreement was very good near the origin, and was poorest at about $S^*=.9$. Further iterations failed to improve the agreement (which is hardly surprising considering

the iteration method used). The values of $\frac{du_c^*}{dS^*}$ and $\frac{1}{M_e}\frac{dM_e}{dS^*}$ found are compared with the direct method results in Figs. 7 and 8. The agreement between $d(\frac{\rho_\infty u_\infty \delta^*}{\sqrt{S_b}})/dS^*$ from Equation 11 with $\Delta(\frac{\rho_\infty u_\infty \delta^*}{\sqrt{S_b}})/\Delta S^*$ from Equation 13 was best near the origin and was poorest at about $S^*=.7$. In the region between the origin and the last point plotted in Figs. 7 and 8, the maximum discrepancy between the two values is $10^o/o$.

It is interesting to note that the direct method solution could not be carried beyond $S^*=.3$ when four significant figures were required of the profiles, while the indirect method, requiring the same number of significant figures, was reasonably accurate to $S^* = .5$. In addition, the errors in agreement between $d(\frac{\rho_\infty u_\infty \delta^*}{\sqrt{S_b}})/dS^*$ and the finite differences derivative appear to be distributed in such a way that the displacement thicknesses far downstream, when calculated in the two different ways as shown in Fig. 6, agree quite well.

The most surprising feature of this method is that it works at all, even without considering the crudness of the iteration scheme. The biggest drawback is that the degree of convergence is limited, but it is possible that this can be improved by refining the iteration procedure.

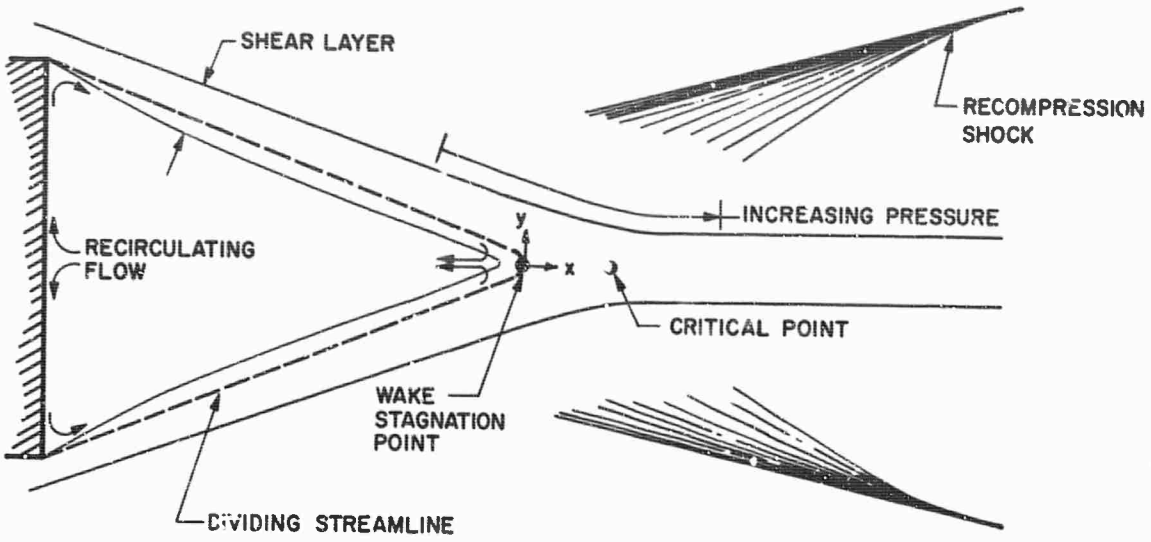

FIG. 1 BASE FLOW REGION

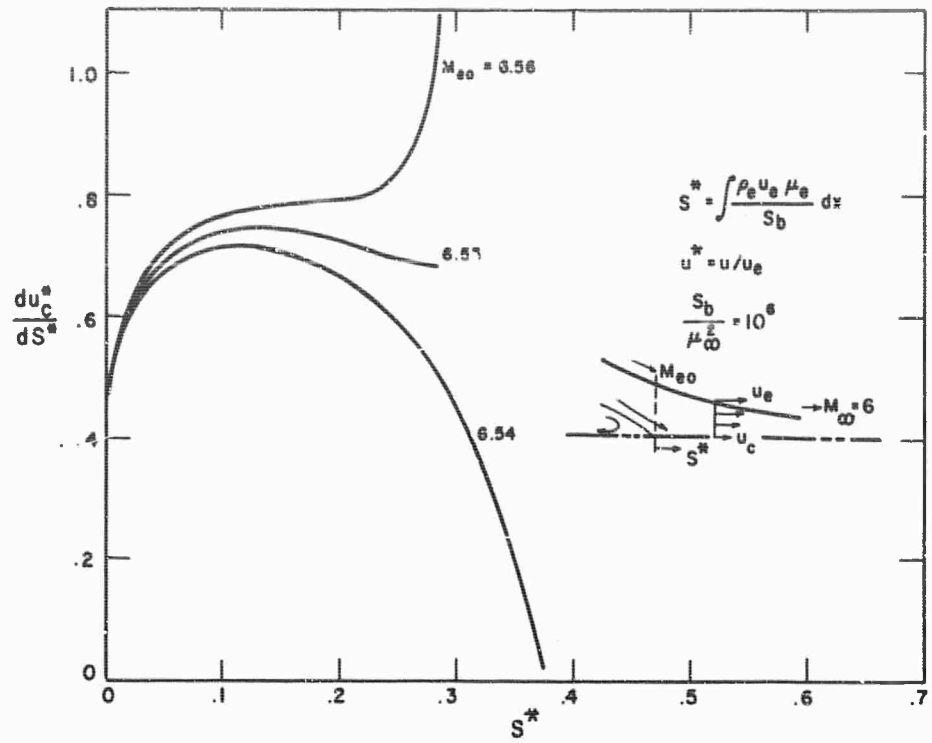

FIG. 2 du_c^*/dS^* FOR M_{eo} CLOSE TO THE EIGENVALUE

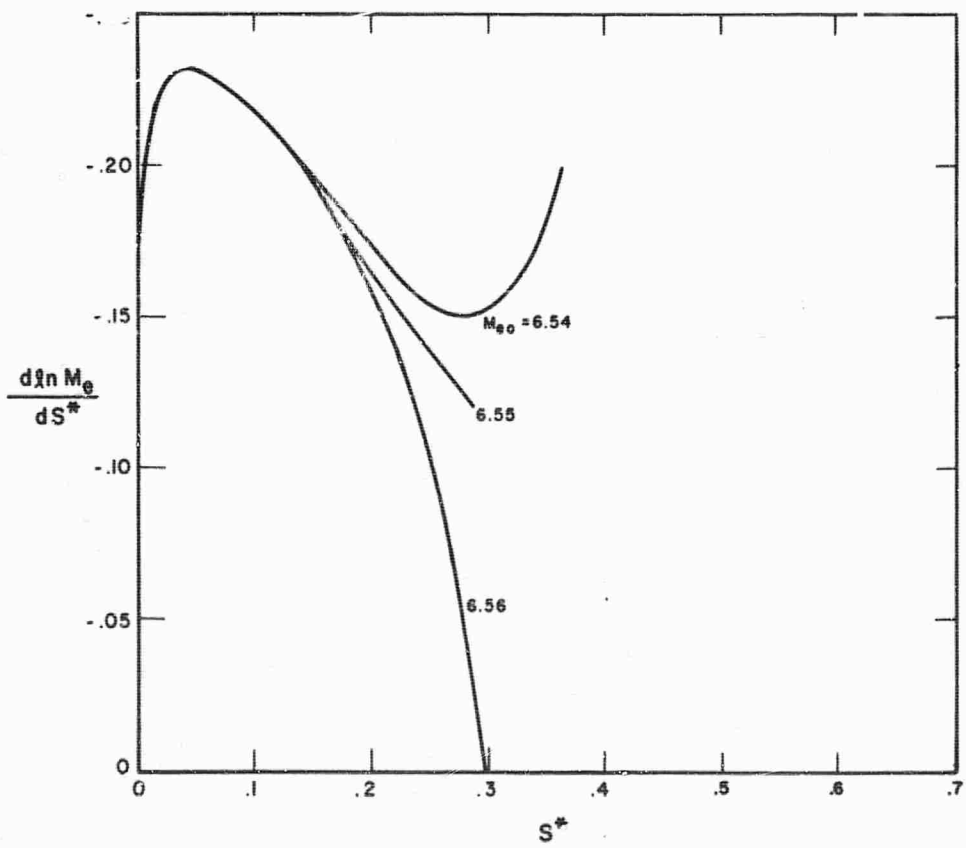

FIG. 3 $d\ln M_e/dS^*$ FOR M_{eo} CLOSE TO THE EIGENVALUE

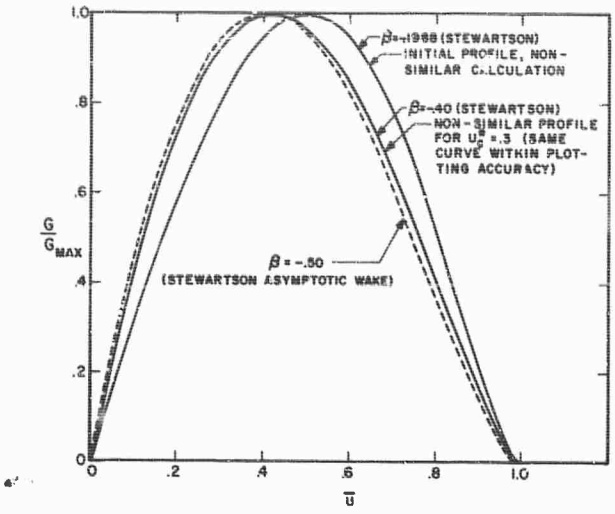

FIG. 4

COMPARISON BETWEEN PROFILE SHAPES FROM THE NON-SIMILAR CALCULATION AND THOSE FROM THE STEWARTSON-KENNEDY SIMILAR SOLUTION

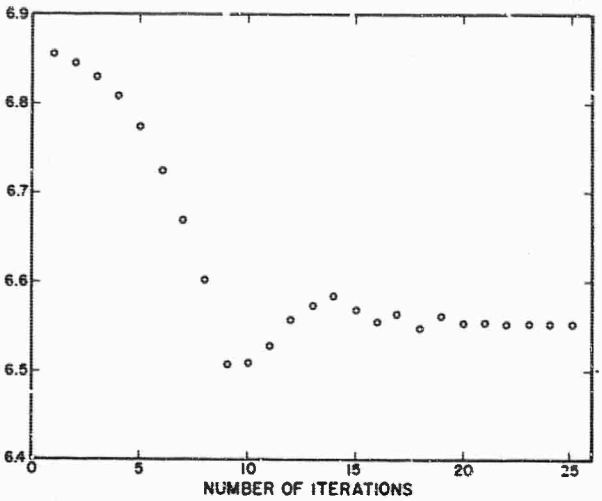

FIG. 5

RATE OF CONVERGENCE TO THE EIGENVALUE

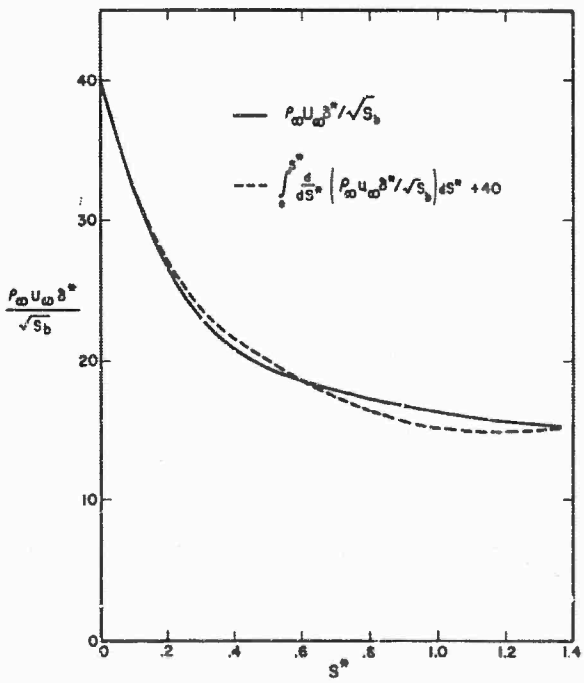

FIG. 6

CONVERGENCE OF INVERSE METHOD, 20 ITERATIONS

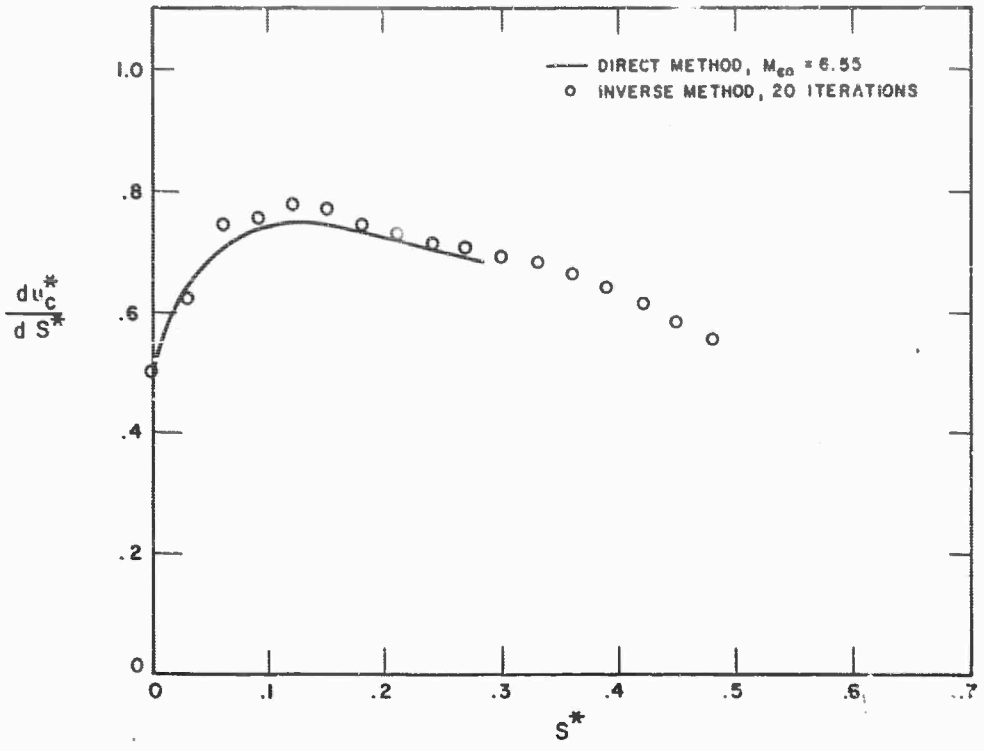

FIG. 7 COMPARISON OF DIRECT AND INVERSE METHODS, du_c^*/dS^*

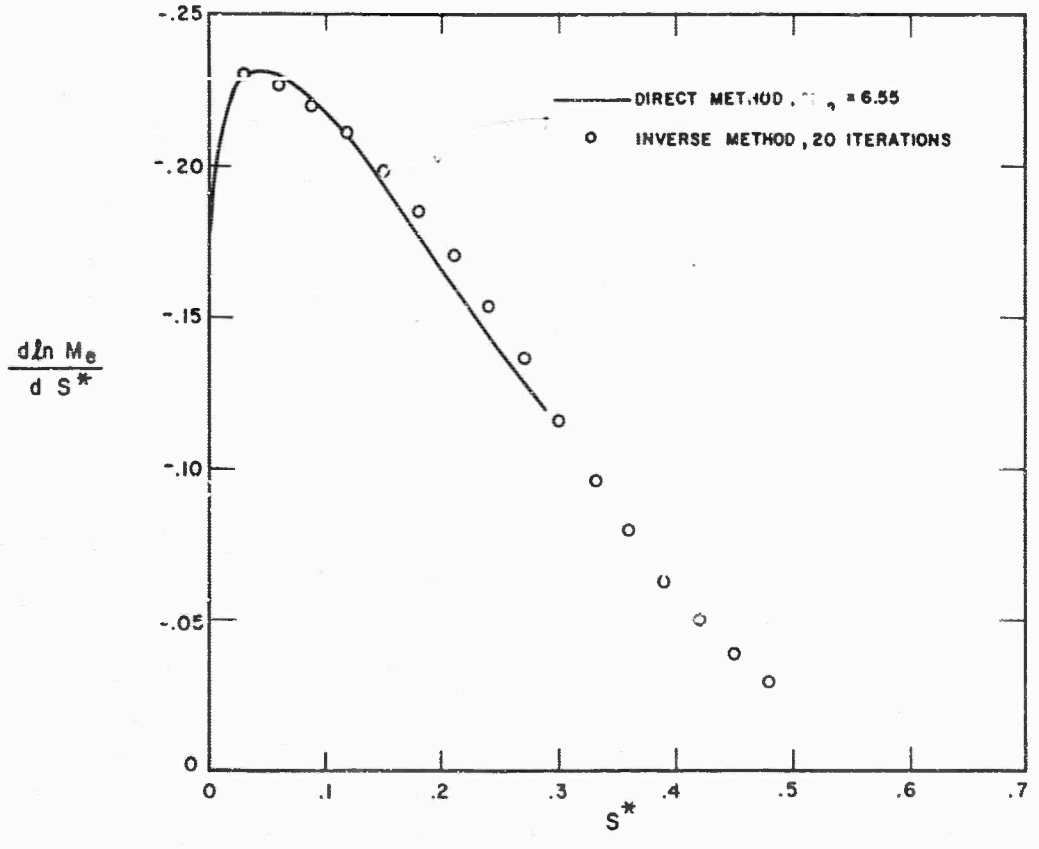

FIG. 8 COMPARISON OF DIRECT AND INVERSE METHODS, $d\ln M_e/dS^*$